Title
A FORM FOR MATTER

Author
Hebert, Alvin J.

Publication Date
1975-09-01

Submitted to Science

LBL-4329 c.1
Preprint

A FORM FOR MATTER

Alvin J. Hebert

October 1975

Prepared for the U. S. Energy Research and
Development Administration under Contract W-7405-ENG-48

A FORM FOR MATTER

by Alvin J. Hebert

Providing a home for the neutrino leads to a theory of gravitational symmetry.

Alvin J. Hebert
PhD in Chemistry

University of California
Lawrence Berkeley Laboratory
Berkeley, California 94720

The Concept

It is suggested that circularization of the Poynting vector of a photon accompanied by half integral helical polarization of the electric and magnetic intensity vectors in a right or left handed mode accounts for the phenomenon of charge and the occurrence of stable matter. Helical polarization can be visualized by considering a Möbius strip with half or whole integral numbers of twists and with the surface of the strip corresponding to the magnetic vector plane of a photon. Möbius strips are shown in Figure 1. The volume swept out by a rotating strip corresponds to a torus, or, if the radius becomes zero, a sphere. An integral helical polarization corresponds to a neutral particle. A half integral change in the helical polarization of a nucleus is considered equivalent to a beta decay or electron capture event, while a whole integral change is considered equivalent to a gamma decay.

This form for electromagnetic energy provides a symmetrical spacial framework for charge, matter and antimatter.

The Hypothesis

If a correlation between nuclear binding energies and helical polarization energies exists, it should allow the formulation of a relationship for the relative abundances of the isotopes. It is therefore hypothesized that helical polarization energy corresponds to neutrino energy and that this energy is retained by a nucleus as binding energy in the beta decay process. To test this hypothesis, the expression

$$N = e^{\frac{E}{T}} \qquad (1)$$

is used to calculate the relative abundance, N, of each stable isotope, where E is a function of the average neutrino energy, and T is a measure of the nuclear temperature. E is calculated from beta decay Q values while T is assumed to be proportional to $|Z - Z_A|$, where Z is the nuclear charge and Z_A corresponds to the point of minimum energy for mass number A in an average neutrino energy versus Z parabola. This is similar to a binding energy versus Z parabola for beta decay(1). It is assumed that the observed beta decay energies extend to or near to a common higher energy continuum which served as a source of the isotopes.

The average neutrino energy is given approximately by

$$E_{\nu\beta^-} = \tfrac{1}{2}(Q_{\beta^-} + .511 \text{ MeV}) \qquad (2)$$

when $Q_{\beta^-} > 1.02$ MeV, and where Q values are given in the Table of Isotopes(2).

$$E_{\nu\beta^-} = \frac{2}{3} Q_{\beta^-} \quad (3)$$

when $Q_{\beta^-} < 1.02$ MeV; and

$$E_{\nu\beta^+} = \frac{1}{2} (Q_{EC} - 1.02 \text{ MeV}) \quad (4)$$

for positron decay when $Q_{EC} > 1.02$ MeV, or

$$E_{\nu EC} = Q_{EC} \quad (5)$$

where Q_{EC} corresponds to an electron capture event. Also,

$$E_{\nu} = \frac{2}{3} Q_{EC} \quad (6)$$

when the decay scheme is complex with roughly 50% β^+ decay, or

$$E_{\nu} = \frac{1}{2} Q_{EC} \quad (7)$$

when the decay scheme is complex and there is roughly 70% β^+ decay; and

$$E_{\nu} = \frac{1}{2} E_{\gamma} \quad (8)$$

where E_γ is the gamma ray energy. Equation (8) is used only where other data are lacking. It corresponds to stating that the recoil momentum of a gamma ray is absorbed by the nucleus.

Equations (2) through (8) were used for the calculations reported here. They were especially useful in cases with complex decay schemes. In spot checks, the values were found to agree well with computer calculations when it was assumed that the average neutrino energy was equal to the Q value minus the average beta energy (3). The agreement was often of the order of 1% for β^- decay and of the order of 1 to 10% for β^+ decay or mixed β^+ and EC events.

A value of Z_A for a stable isotope is obtained by establishing the minimum energy point in a Z versus $\sqrt{E}$ parabola, or

$$Z_A = \frac{Z_{\beta+} + Z_{\beta-}\sqrt{E_{\nu\beta+}/E_{\nu\beta-}}}{1 + \sqrt{E_{\nu\beta+}/E_{\nu\beta-}}} . \qquad (9)$$

In the cases of He^3, Li^6, Li^7 and O^{16}, Fermi's formula

$$Z_A = \frac{A}{1.98 + .015\,A^{2/3}} \qquad (10)$$

was used to estimate Z_A.

The temperature for a given transition is taken as

$$T_Z = |Z - Z_A| \qquad (11)$$

where Z corresponds to the nuclear charge of the isotope prior to decay.

Each neutrino energy divided by its transition temperature is then added to any other isotope, i, on the same side of Z_A to give the sum

$$S = \sum_i \left[\frac{E_\nu}{T_Z}\right]_i \quad . \qquad (12)$$

One value of S is thus obtained for the sum of $\left[E_\nu / T_Z\right]_i$ values for β^- transitions, and a second for the sum over β^+ or EC transitions.

The quantity T is introduced to provide a temperature normalization among the stable isotopes,

$$T = \sqrt{\frac{\dfrac{(\text{B.E. at Ni}^{62})}{62}}{\dfrac{(\text{B.E. for stable isotope i})}{A_i}}} \qquad (13)$$

where the binding energies, B.E., have been tabulated by Wapstra(4). For most isotopes this corresponds to a small (less than 5%) correction to the nuclear temperature.

The abundance of a stable isotope is then given by

$$N = 10^{\frac{S}{T}} \tag{14}$$

which is equivalent to equation (1) with $S = E/2.303$. The larger of the two usual beta decay summations is then used for abundance calculations.

Isotopic and Elemental Abundances

The results for the abundances of the isotopes are shown in Table 1 along with observed relative terrestrial abundances(2). The agreement between observed and calculated relative abundances for many of the isotopes is good considering the range of the values, the accuracy and completeness of the data, and the simplifying assumptions used.

The hypothesis is further tested by comparing reported cosmic elemental abundances(6) with those calculated from the isotopic abundances given in Table 1. The results are shown in Figure 2 where the data have been shifted to agree at a silicon (Si) abundance of 10^4. Here both the pattern and the magnitudes of differences between most neighboring elements are in good agreement. The agreement for the light major elements is, in several cases, exceptional. The temptation to introduce a parameter to obtain better agreement for the heavier elements was abated by also plotting values in Figure 2 for a well studied type Ap star, α^2 Canum Venaticorum (α^2CVn) as given relative to normal stars(7). Isotopes with the same A in most cases have a partitioning of abundances that favors the greatest $\log_{10}N$, in agreement with theory. The effect of this on calculated relative abundances has not been included.

Form, Charge, and Magnetic Moments

The magnetic moments of the neutron, the proton, and the electron have been measured very accurately. Therefore they are used here to provide a more rigid test for the suggested form.

It is hypothesized that the magnetic moment of the neutron arises from two resonant charge modes where the positive mode is shielded in a transverse resonance so as to appear stationary with respect to the spinning negative mode. At the instant of neutron decay, the outer toroidal negative surface begins converting to a spherical mode that is emitted as an electron, leaving behind a spinning toroidal proton.

A torus with equal radii of revolution and cross-section is shown in Figure 3. The spherical electron mode is assumed to have the same radius. The surface area of the torus is $4\pi^2r^2$. The surface area of the sphere is $4\pi r^2$. Assuming that the magnetic moments are proportional to charge surface area gives $4\pi^2r^2/4\pi r^2 = \pi$ for the proton-electron ratio, and $-\frac{1}{2}(4\pi^2r^2)/4\pi r^2 = -\frac{1}{2}\pi$ for the neutron-electron ratio. The unit spherical electron moment is initially uncorrected for mass differences. The factor $-\frac{1}{2}$ for the neutron is interpreted as the ratio of charged spinning surfaces to number of surfaces, with the minus sign denoting a charged surface arising from an even number of surfaces in transverse modes.

The experimental values are $\mu_p = 2.79278217$ for the proton and $\mu_n = -1.91314886\underline{6}$ for the neutron in nuclear magnetons, where the underlined digits correspond to the error at the positions to their left; $e\hbar/2 m_p c$ is one nuclear magneton, e is the electron charge, $\hbar$ is Plancks constant divided by 2π, m_p is the proton mass, and c is the velocity of light (5), (8). The magnetic moment of the electron is reported as $\mu_e = 1.0011596447$ Bohr magnetons, $e\hbar/2 m_e c$, where m_e is the electron mass(5).

The discrepancies between these values and the above theoretical ones are of the order of 10%. However, the sum of the theoretical absolute values of the proton and neutron moments, $(3/2)\pi$, yields excellent agreement (at the .001% level) with the experimental absolute value sum in neutron magnetons, $e\hbar/2 m_n c$, where m_n is the neutron mass. This suggests a single correction moment which adds to the theoretical neutron moment and subtracts from the theoretical proton moment. An empirical correction moment that will give good results can be calculated from either of the experimental moments, or from their experimental ratio, however a value deduced from the geometry of the situation is preferred.

It is assumed that the theoretical neutron magnetic moment is increased by a latent electron contribution that slightly changes the effective surface area. The correction moment is assumed equal to the product of the sphere to torroidal neutron charged surface area ratio, $2/\pi$, and the scaling factor $\sqrt[3]{1/2\pi}$ where $1/2\pi$ is the doubled volume of a neutron torus with radii $1/2\pi$ and two unit surface areas. The value $1/2\pi$ also corresponds to the change in apparent radius of a unit circumference Möbius loop in changing from an even to odd or from odd to even helical polarization mode. The correction moment is then given as

$$\mu_c = \frac{2}{\pi}\sqrt[3]{\frac{1}{2\pi}} \text{ neutron magnetons} \quad (15)$$

$$= 0.3450008514 \text{ neutron magnetons .}$$

The theoretical moments and experimental values for comparison are given in the following summary:

theoretical

$$\mu_p = \pi - \mu_c \text{ neutron magnetons} \quad (16)$$

$$= 2.796591802 \text{ neutron magnetons}$$

$$\mu_p m_p / m_n = 2.792732559 \text{ nuclear magnetons}$$

experimental

$$\mu_p = 2.79278\underline{217} \text{ nuclear magnetons}$$

theoretical

$$\mu_n = -\left[\frac{\pi}{2} + \mu_c\right] \text{ neutron magnetons} \qquad (17)$$

$$= -1.915797178 \text{ neutron magnetons}$$

$$\mu_n m_p / m_n = -1.913153414 \text{ nuclear magnetons}$$

experimental

$$\mu_n = -1.913148\underline{66} \text{ nuclear magnetons}$$

The ratio of the neutron to proton magnetic moments has been measured. The value reported by Ramsey(8) is

$$\left|\frac{\mu_n}{\mu_p}\right| = 0.685039\underline{17} ;$$

the present theoretical value is

$$\left|\frac{\mu_n}{\mu_p}\right| = 0.6850471263 .$$

Any inaccuracy in the theoretical correction moment would be most sensitively detected by the experimental ratio.

The electron moment initially inferred from the above ratios is

$$\mu_e \frac{m_e}{m_n} = 1 \text{ neutron magneton} \qquad (18)$$

or,
$$\mu_e = 1 \text{ Bohr magneton.}$$

A correction moment for the electron is expected to add to this value and is taken as equal to the charge to magnetic flux quantum ratio

$$\frac{e}{hc/e}$$

and thus,
$$\mu_e = 1 + \frac{e}{hc/e} \text{ Bohr magnetons} \qquad (19)$$

$$= 1.00116141 \text{ Bohr magnetons}$$

while the reported value is

$$\mu_e = 1.001159644\underline{7} \text{ Bohr magnetons}(5).$$

The charge to magnetic flux quantum ratio is usually given as $\alpha/2\pi$ and is the correction term given by Schwinger in his relativistic quantum electrodynamics theory for the anomalous electron moment(9). It is reported in the above manner for reasons to be given later in this paper.

Gravitational and Nuclear Binding Energy

The suggested form for matter is assumed to give rise to large attractive forces near the center of the torus, such as shown in Figure 3. Charge occurs around the center of the circularized rotating electric and magnetic vectors. The central area may be very small or a region of slightly overlapping intensity vectors. Equality is assumed between the rest mass energy, E_r, and the gravitational energy, E_g,

$$\frac{E_r}{E_g} = \frac{2\,m\,c^2}{G\,m^2/\,r_i} = 1 \qquad (20)$$

where m is the mass of a particle, G is the gravitational constant, c is the velocity of light and r_i is the radius of the central or inner torus area. For a proton, Equation (20) gives

$$r_i = Gm/2c^2 = 6.21 \times 10^{-53} \text{ cm} . \qquad (21)$$

This is equivalent to stating that the relativistic gravitational red shift $\delta\nu$, of frequency ν is(9)

$$\delta\nu = \frac{Gm}{rc^2}\,\nu = 2\,\nu \qquad (22)$$

which is the expected symmetrical red shift plus blue shift for a circularized photon with centrally intersecting or closely interacting intensity vectors.

The ratio of the energy of a photon, E_p, with a wavelength λ corresponding to r_i, to the rest mass energy of a proton, E_r, is

$$\frac{E_p}{E_r} = \frac{h\nu}{m c^2} = \frac{hc}{m c^2 \lambda} = \frac{hc}{m c^2 (G m/2 c^2)} = \frac{2hc}{G m^2} \quad (23)$$

where m is the proton mass and h is Plancks constant. Inserting the constants yields

$$\frac{E_p}{E_r} = 2.13 \times 10^{39}$$

The ratio of the electrostatic or charge energy, E_e, of a sphere to the gravitational energy, E_g, of a proton at the same radius is

$$\frac{E_e}{E_g} = \frac{e^2}{G m^2} = 1.236 \times 10^{36} . \quad (24)$$

From equations (23) and (24) the photon to charge energy ratio for a gravitationally bound particle is therefore

$$\frac{E_p}{E_e} = \frac{2hc}{e^2} = 1722.045 \quad (25)$$

or $4\pi/\alpha$ where α is the fine structure constant. Multiplying this ratio by the ratio of the electron radius, $r_e = e^2/2m_ec^2$, to the Compton radius for a proton, $r_p = h/m_pc$ gives

$$\frac{E_pr_e}{E_er_p} = \frac{2hc}{e^2} \cdot \frac{e^2}{2m_ec^2} \cdot \frac{m_pc}{h} = \frac{m_p}{m_e} \qquad (26)$$

This is an expected partitioning ratio for energy, but it corresponds to a 7% change in radius or energy ratio from equation (25). The change is close to the ratio of the correction moment, μ_c, to the change in nuclear magnetic moment, $(3/2)\pi$, in neutron decay, thus lending additional weight to the theory that the neutron is larger with respect to electrostatic energy or effective surface area than the proton.

Fundamental Constants and Ratios

Dixon has shown that mass ratios of the proton, the neutron, the electron and the strange particles may be obtained as integers from values of a hyperbolic sine function where a base number for the electron is taken as 2^6 or $64_{(10)}$. He gives no reason for the striking agreements. The torus shown in Fig. 3 has a radius defined by

$$r = \frac{a}{\sinh \eta} \tag{27}$$

in toroidal coordinates where a is a constant. The present theory thus predicts a strong correlation between fundamental physical constants or ratios and the hyperbolic sine function especially for $r = 1/2\pi$ where arcsinh $2\pi = 2.5372975$, a value that may serve as the ratio of the neutron-proton mass difference to the electron mass. With respect to the Dixon base of 2^6 for the electron mass, it is found that

$$\frac{\sinh(2^6)}{\sinh(3^2 \cdot 2\pi)} = 1722.156, \tag{28}$$

a ratio very close to that given by equation (25), and corresponding to a value of 1/137.045 for the fine structure constant.

It is noted that sinh $2\pi = 267.7$, which is close to the average pion to electron mass ratio. It is also noted that $\sinh x = \sinh(x + 2\pi i)$, which should be of help in understanding charge and its relationship to the mathematical concept i.

A value for Avogadro's number, N, is also found at the 18π resonance

$$N = \frac{1}{3}\sinh(3^2 \cdot 2\pi) = 6.034 \times 10^{23} \text{ mole}^{-1} \quad (29)$$

where the number 3 may denote the number of dimensions that the particle in question requires. This value for N is thought to correspond to a neutron mass scale and division by the factor $(m_n/m_p)(1 + m_e/m_p) = 1.00192727$, gives $N = 6.02264 \times 10^{23}$ mole^{-1}, in agreement with the unified mass scale value of $6.02252\underline{9} \times 10^{23}$ mole^{-1}(2).

The assumption of equality between rest mass energy and gravitational energy led to Eqn. (21) and an inner torus radius r_i proportional to G, the gravitational constant. It is expected that a ratio involving so fundamental a dimension should be present as a resonance value. This would provide a theoretical value for G and perhaps shed more light on the subject of gravitation and its relationship to the present form. The necessary value is obtained at the $2^5\pi$ or 32π resonance. The radius in Eqn. (21) is then obtained from an intuitive match as a ratio

$$\frac{r_i}{r_p} = \frac{2\pi}{\sinh(32\pi)} \cdot \frac{r_p}{r_e} \cdot \frac{1}{m_e N} \quad . \tag{30}$$

Inserting the equations for r_p and r_e, equating r_i to Eqn. (21) and solving for G yields

$$G = \frac{32\pi}{\sinh 32\pi} \cdot \frac{1}{(m_p)^3 N} \cdot \left(\frac{hc}{2e}\right)^2 \tag{31}$$

and,

$$G = 6.6741 \times 10^{-8} \text{ dyne cm}^2 \text{ g}^{-2}$$

when the unified mass scale value of N is used, and

$$G = 6.670319335 \times 10^{-8} \text{ dyne cm}^2 \text{ g}^{-2}$$

when the value $N = \frac{1}{3}\frac{m_p}{m_n}\sinh(18\pi) = 6.02592 \times 10^{23}$ mole^{-1} is used. The experimental value is

$$G = 6.670\underline{5} \times 10^{-8} \text{ dyne cm}^2 \text{ g}^{-2} \quad ,$$

and thus both calculated values are within the experimental error.

In superconductor theory the magnetic flux in the hole of a ring or torus is an integral multiple of $(hc/2e)$ where hc/e is the quantum of magnetic flux. The quantity $(hc/2e)^2$ is proportional to the free energy for charged superconducting particles(11). Occurrence of this quantity in Equation (31) suggests a connection between gravity, which is the nuclear force, and magnetic flux quanta. Magnetic flux quanta should fit nicely into a torus with a helically spinning superconducting charged surface, a surface that repels magnetic fields. This would be in keeping with the symmetry in nature, with like units of charge being repulsive and like units of magnetic flux attractive.

The symmetry of charge conservation suggests a second magnetic flux quantum that conserves gravitation and is repelled by the first. The electron has a tendency to fly out of neutrons and it thereafter spends very little, if any, time in a proton. It is thus regarded as a prime candidate for possessing antigravity magnetic flux quanta.

Summary and Conclusions

In many cases the predicted values for isotopic and elemental abundances are unsatisfactory. This could be due to several inadequacies, and experimental checks on the isotopes of a few elements such as nitrogen, oxygen, sulfur, calcium, barium and osmium should serve to fine tune the theory. Discrepancies could then be easily checked experimentally with predicted decay energies arrived at from measured abundances.

A fine tuned theory may lead to accuracies which will allow predictions of the age of the elements, with cross checks between elements such as strontium and rubidium or rhenium and osmium. The present predicted abundances for the uranium isotopes give an age of 5×10^9 years when the gamma ray data are used for both isotopes, and a value of 6×10^9 years when the beta decay data for U^{235} are used.

The mass deficit evident in Figure 2 for the observed heavy elements is quite close to the mass excess observed above the theoretical values for manganese, iron and nickel. The drop in uranium abundance would cause an almost complete loss of U^{235} if natural decay occurred smoothly, so a different process is called for if the heavy elements are to convert to iron over the same time span and without affecting isotope ratios. One answer is in an explosion 6×10^9 years ago that converted heavy elements to iron, followed by re-equilibration of the remaining heavy elements in a high energy continuum. This is equivalent to time zero plus more iron and less heavy elements in a closed system.

The nuclear magnetic moments predicted from the geometrical considerations of this theory are in excellent agreement with measured values. The predicted magnetic moment for the electron is in agreement with the reported value to within 2 parts in 10^6. This is as expected because the same correction moment is used here for the electron and in quantum theory. The reported value has an accuracy of 7 parts in 10^9. The correction term used here, e^2/hc, is given as a mass ratio and can be thought of as the ratio of unit charge to unit magnetic flux. It is expected that better agreement will be obtained when further gravitational and antigravitational corrections are made.

It is concluded that the anomalous electron magnetic moment arises from a mass effect. The fact that the observed laboratory electron magnetic moment corresponds to what would be expected for a lighter electron supports this.

The gravitational theory presented here is further supported by considering the energy necessary to transport an electron from a hydrogen atom to infinity as compared to the energy necessary to transport an electron from an infinite mass hydrogen atom to infinity. The difference is very small and is in direct conflict with gravitational considerations if the electron has normal gravitational mass. The difference is $R_\infty - R_H$, where R_∞ is the Rydberg constant for an infinite mass hydrogen and R_H is the Rydberg constant for hydrogen. The difference is due to the appropriately named reduced mass term

$$\frac{m_e m_p}{m_e + m_p}$$

and is very close to the value $R_\infty m_e/m_p$, and within $2r_e/R_\infty r_p$ of $\alpha/2\pi$. Taking the charged proton mass as zero in a standard derivation for the hydrogen atom(12) yields an energy to transport the electron to infinity of R_∞. This is greater than R_H which contains the reduced mass term. This is not in conflict with gravitational considerations. Thus it is demonstrated that more energy is required to transport an electron from a zero mass charged proton to infinity than from a proton possessing mass and charge to infinity. The electron exhibits a reduced mass in the spectra of the hydrogen atom and with respect to its magnetic moment. This is a result of the symmetry of charge, where opposites attract and likes repel, and of the symmetry of gravitational magnetic flux quanta where likes attract and opposites repel.

If two electrons can be in a common symmetrical non-repulsive environment with respect to charge, they should couple or pair gravitationally as in molecules, with an energy corresponding to the reduced mass. An analogous situation occurs in helium where two protons pair in the environment of two neutrons and two electrons.

A reassuring proof for these gravitational considerations is provided by inspection of Table 7-1 on page 216 of Semat's Introduction to Atomic and Nuclear Physics(12), where the dependence of the Rydberg constant on the mass of the nucleus has been tabulated. It is apparent that the addition of a neutron, with its latent electron, to the proton nucleus, gives rise to a measured increase over the calculated theoretical electrostatic energy necessary to remove an electron to infinity with no increase in electrostatic charge. The same occurs in the case of ${}_3Li^6$ and ${}_3Li^7$, but the increase in energy is smaller.

In conclusion, the suggested form for matter has provided methods for calculating isotopic abundances, magnetic moments, some fundamental ratios in nature, and a theory of gravitational symmetry. It has been demonstrated that helical polarization energy is equivalent to neutrino energy, to nuclear binding energy, to gravitational energy, and to magnetic flux quanta energy.

References

1. G. Friedlander and J.W. Kennedy, Nuclear and Radiochemistry, (Wiley, New York, 1957).
2. C.M. Lederer, J.M. Hollander, I. Perlman, Table of Isotopes, Sixth Edition, (Wiley, New York, 1967).
3. Private Communication, C.M. Lederer.
4. A.H. Wapstra, Atomic Masses of Nuclides, in Encyclopedia of Physics, 38/1, (Springer-Verlag, Berlin, Gottinger, Heidelberg, 1958) pp. 6-13.
5. H. Rittenberg, A. Barbaro-Galtieri, T. Lasinski, A.H. Rosenfeld, T.G. Trippe, M. Roos, C. Brieman, P. Soding, N. Barash-Schmidt, C. Wohl, Rev. Mod. Phys., 43, S14 (1971).
6. H.C. Urey, Phys. Rev., 88, 248 (1952).
7. E.M. Burbidge, G.R. Burbidge, W.A. Fowler, F. Hoyle, Rev. Mod. Phys., 29, 630 (1957). W.L.W. Sargent, Ann. Rev. Astronomy Astrophys., 2, 297 (1964). P.J. Brancazio and A.G.W. Cameron, Can. J. Phys., 45, 3297 (1967).
8. N. F. Ramsay, Molecular Beams, (Oxford Press, London, 1956), p. 285
9. J. Schwinger, Phys. Rev., 73, 416 (1948). J. Schwinger, Phys. Rev., 76, 790 (1949).
10. G. Dixon, Particles and Nuclei, 5, 23 (1973).
11. G. Rickayzen, Theory of Superconductivity, (Interscience Publishers, a division of John Wiley and Sons, New York, London, Sydney, 1965), p. 299.

12. L. Pauling and E.B. Wilson, Jr., Introduction to Quantum Mechanics, (McGraw-Hill Book Co., Inc., New York, London, 1935). H. Semat, Introduction to Atomic and Nuclear Physics, (Reinhart and Co., Inc., New York, 1958).

13. Work performed under the auspices of the United States Energy Research and Development Administration.

14. Acknowledgments

Acknowledgements

I thank my wife Marie for her help in preparing this manuscript, and I thank my father Antonio who always tells me, "Everything works together!".

CAPTION FOR TABLE 1

Log_{10} N values that involve particle unstable states are given in parentheses and are not used for relative abundance calculations. A few with parentheses are based on estimates and are not used for calculations. Helium was included for completeness, as was hydrogen. A Q value for hydrogen was estimated from the Σ^0 decay data(5). Values calculated from E_γ are underlined. A + beside a value corresponds to a decay scheme which has a missing transition energy.

0 0 0 0 4 4 0 3 9 9 5

TABLE 1

LOG ISOTOPIC ABUNDANCES (Log_{10} N) AND ISOTOPIC PERCENTAGES

Isotope	Calculated Log_{10} N		Calculated Percentage	Terrestrial Percentage[2]
H^1	(162)		100	100
H^2				.015
He^3	.004		10^{-7}	10^{-4}
He^4	(10.3)	(7.8)	100	100
Li^6	.53		68	7.4
Li^7		.20	32	92.6
Be^9	.72			100
B^{10}	.54	.85	.3	20.0
B11	3.42	.97	99.7	80.0
C^{12}	7.40	7.34	99.9	98.9
C^{13}	4.16	4.01	.06	1.1
N^{14}	6.16	1.16	99.8	99.6
N^{15}	3.39	1.4	.2	.4
O^{16}	7.52		99.9	99.8
O^{17}	3.10	3.10	.004	.04
O^{18}	4.10	2.05	.05	.2

F^{19}	2.07	1.33		100
Ne^{20}	5.27	5.46	95.4	91
Ne^{21}	2.42	2.26	.09	.03
Ne^{22}	4.14	1.58	4.6	8.8
Na^{23}	2.10	1.66		100
Mg^{24}	4.40	5.29	79.8	78.8
Mg^{25}	1.96	4.67	19.1	10.2
Mg^{26}	3.45	3.13	1.1	11.1
Al^{27}	1.60	1.76		100
Si^{28}	3.87	5.11	92.5	92
Si^{29}	2.02	3.88	5.5	4.7
Si^{30}	3.16	3.45	2.0	3.1
P^{31}	1.22	1.81		100
S^{32}	1.85	4.27	96.5	95
S^{33}		2.37	1.2	.8
S^{34}	2.65	2.39	2.3	4.2
S^{36}		.56	.019	.015

Cl^{35}		1.47	21.6	75.6
Cl^{37}	2.03	(3.49)	78.4	24.5
Ar^{36}	.23		.02	.3
Ar^{38}	3.44	4.00	86.6	.06
Ar^{40}	3.19	1.96	13.4	99.6
K^{39}	1.96	1.85	86.8	93
K^{40}			0	.12
K^{41}	1.14	(2.79)	13.2	6.8
Ca^{40}	1.67	4.54	97.3	97
Ca^{42}	2.42	2.68	1.4	.6
Ca^{43}	.99	2.27	.5	.15
Ca^{44}	2.43	1.73	.8	2.1
Ca^{46}			0	.003
Ca^{48}			0	.2
Sc^{45}	1.77	.72		100
Ti^{46}	1.75	2.53	4.0	8
Ti^{47}	2.37	.78	2.7	7.5
Ti^{48}	2.03	2.40	3.0	74
Ti^{49}	2.39	1.16	2.9	5.5
Ti^{50}	3.87	1.84	87.4	5.3

V^{50}			0	.3
V^{51}	1.27	1.40	100	99.8
Cr^{50}	.99	1.18	2.6	4.3
Cr^{52}	2.19	2.69	82.7	84
Cr^{53}	1.55	1.71	8.6	9.6
Cr^{54}	1.55	1.45	6.1	2.4
Mn^{55}	1.07	1.53		100
Fe^{54}		2.45	22.7	5.8
Fe^{56}	2.69	2.86	58.3	91.7
Fe^{57}	1.36	1.79	5.0	2.2
Fe^{58}	1.45	2.24	14.0	.3
Co^{59}	1.04	2.02		100
Ni^{58}		2.38	27.7	68
Ni^{60}	1.92	2.31	23.5	26.2
Ni^{61}	2.06	2.12	15.2	1.3
Ni^{62}	2.46	2.40	33.2	3.7
Ni^{64}		.56	.4	1.2
Cu^{63}	1.69	1.54	75.5	69.1
Cu^{65}	1.20	(2.72)	24.5	30.9

Zn^{64}	.73	2.05	5.4	49
Zn^{66}	1.86	3.24	84.0	27.8
Zn^{67}	1.68	1.94	4.2	4.1
Zn^{68}	2.12	1.67	6.4	18.6
Zn^{70}			0	.6
Ga^{69}	.98	1.97	51.8	60.2
Ga^{71}	1.08	1.94	48.2	39.8
Ge^{70}	1.39	2.15	14.3	20.6
Ge^{72}	2.39	2.50	32.0	27.4
Ge^{73}	.82	1.29	2.0	7.7
Ge^{74}	2.64	1.99	44.2	36.7
Ge^{76}	1.87		7.5	7.7
As^{75}	1.72	1.88		100
Se^{74}	1.09	1.40	3.0	.9
Se^{76}	1.87	(2.73)	8.8	9.0
Se^{77}	1.15	1.83	8.1	7.6
Se^{78}	2.38	1.52	28.6	23.5
Se^{80}	2.63	1.63	50.9	49.8
Se^{82}	.7		.6	9.2
Br^{79}	1.14	.70	20.4	50.5
Br^{81}	1.73	1.30	79.6	49.5

Kr^{78}			0	.35
Kr^{80}	1.70	.72	10.4	2.3
Kr^{82}	1.74	1.80	12.9	11.6
Kr^{83}	1.54	1.24	7.1	11.6
Kr^{84}	2.38	1.98	49.2	56.9
Kr^{86}	2.0		20.4	17.4
Rb^{85}	1.54	1.57	5.5	72.1
Rb^{87}	2.81	1.49	94.5	27.9
Sr^{84}	.65	.90	.08	.6
Sr^{86}	1.57	3.23	17.4	9.9
Sr^{87}	3.21	2.01	16.6	7.0
Sr^{88}	3.54	3.81	66.0	82.6
Y^{89}	3.27	3.06		100
Zr^{90}	3.85	3.14	40.0	51.5
Zr^{91}	3.36	2.09	13.0	11.2
Zr^{92}	3.91	1.86	46.0	17.1
Zr^{94}	2.04		.6	17.4
Zr^{96}	1.84		.4	2.8
Nb^{93}	2.73	2.33		100

Mo^{92}		1.71	9.7	15.9
Mo^{94}	1.59	2.36	43.4	9.1
Mo^{95}	1.87	1.63	14.0	15.7
Mo^{96}	1.72	1.57	10.0	16.5
Mo^{97}	1.57	1.57	7.1	9.5
Mo^{98}	1.60		7.5	23.8
Mo^{100}	1.64		8.3	9.6
Ru^{96}			0	5.5
Ru^{98}	1.20	1.44	2.6	1.9
Ru^{99}	1.66	1.51	4.3	12.6
Ru^{100}	2.05	2.52	31.0	12.5
Ru^{101}	1.57	1.25	3.5	17.0
Ru^{102}	2.76	2.16	53.8	31.6
Ru^{104}	1.71	1.17	4.8	18.9
Rh^{103}	1.20	1.36		100
Pd^{102}	1.25	(2.57)	2.4	.96
Pd^{104}	1.51	2.16	19.7	11.0
Pd^{105}	1.82	1.55	9.0	22.2
Pd^{106}	2.03	1.97	14.6	27.3
Pd^{108}	2.51	1.52	44.1	26.7
Pd^{110}	1.73	1.87	10.1	11.8

Ag^{107}	1.73	1.59	68.1	51.4
Ag^{109}	1.13	1.40	31.9	48.6
Cd^{106}		.90	1.9	1.2
Cd^{108}	1.29	1.20	4.6	.9
Cd^{110}	1.73	1.87	17.5	12.4
Cd^{111}	1.42	1.63	10.0	12.8
Cd^{112}	2.18	1.83	35.7	24.1
Cd^{113}	.75		1.3	12.3
Cd^{114}	2.04	1.22	25.8	28.9
Cd^{116}	1.13		3.2	7.6
In^{113}	1.04	1.55	65.1	4.2
In^{115}	1.28+		34.9	95.8
Sn^{112}	.46		.03	1.0
Sn^{114}	1.52	1.12	.4	.7
Sn^{115}	1.90	2.30	2.3	.3
Sn^{116}	2.14	3.45	32.8	14.2
Sn^{117}	1.94	2.30	2.3	7.6
Sn^{118}	2.44	3.66	53.1	24.0
Sn^{119}	2.08	.75	1.4	8.6
Sn^{120}	2.78	2.36	7.0	33.0
Sn^{122}	1.20	1.56	.4	4.7
Sn^{124}	1.32		.2	6.0

Sb^{121}	1.61	2.20	69.6	57.3
Sb^{123}	1.54	1.84	30.4	42.8
Te^{120}		1.25	2.6	.1
Te^{122}	1.56	1.71	7.6	2.5
Te^{123}		1.84	10.2	.9
Te^{124}	1.69	1.97	13.7	4.6
Te^{125}	1.00	1.68	7.0	7.0
Te^{126}	1.98	1.55	14.1	18.7
Te^{128}	2.45	1.48	41.5	31.8
Te^{130}	1.35+		3.3	34.5
I^{127}	1.86	1.35		100
Xe^{124}			0	.1
Xe^{126}	.96	1.32	3.2	.1
Xe^{128}	1.44	2.08	18.4	1.9
Xe^{129}	1.48	2.20	24.3	26.4
Xe^{130}	1.77	1.89	11.9	4.1
Xe^{131}	1.76	1.87	11.4	21.2
Xe^{132}	2.07	1.79	18.0	26.9
Xe^{134}	1.15+		2.2	10.4
Xe^{136}	1.84		10.6	8.9
Cs^{133}	1.24	1.24		100

Ba^{130}	.28	.81	.7	.1
Ba^{132}	.89	.90	.8	.2
Ba^{134}	.83	2.04	11.2	2.6
Ba^{135}	1.39	1.16	2.5	6.7
Ba^{136}	1.59	1.78	6.1	8.1
Ba^{137}	1.77	1.80	6.4	11.9
Ba^{138}	2.85	1.35	72.2	70.4
La^{138}			0	.09
La^{139}	2.56	2.34	100	99.9
Ce^{136}		.7	.7	.2
Ce^{138}	.96	1.12	1.7	.25
Ce^{140}	(3.59)	2.84	91.4	88.4
Ce^{142}	1.67		6.2	11.07
Pr^{141}	2.12	2.01		100
Nd^{142}	1.45	1.77	5.3	27.1
Nd^{143}	1.59	1.92	7.4	12.2
Nd^{144}	2.80	1.52	56.4	23.9
Nd^{145}	1.37	2.22	14.8	8.3
Nd^{146}	2.21	1.19	14.5	17.8
Nd^{148}	1.22		1.5	5.7
Nd^{150}			0	5.6

Sm^{144}		1.29	8.0	3.2
Sm^{147}	1.28	1.36	9.4	15.1
Sm^{148}	1.58	(1.86)	15.6	11.3
Sm^{149}	1.20	.98	6.5	13.8
Sm^{150}	1.79	1.56	25.2	7.5
Sm^{152}	1.72	1.33	21.5	26.6
Sm^{154}	1.53		13.9	22.5
Eu^{151}	1.15	1.47	49.4	47.8
Eu^{153}	.96	1.48	50.6	52.2
Gd^{152}	1.50	(3.68)	17.9	.2
Gd^{154}	1.41	(1.91)	14.5	2.2
Gd^{155}	.85	1.03	6.1	15.0
Gd^{156}	1.76	1.52	32.6	20.5
Gd^{157}	.57	.78	3.4	15.7
Gd^{158}	1.54	.91	19.6	24.7
Gd^{160}	1.02		5.9	21.6
Tb^{159}	.99	.94		100
Dy^{156}		.46	.7	.06
Dy^{158}	.82	.71	1.5	.1
Dy^{160}	1.34	2.19	36.0	2.3
Dy^{161}	1.19	1.99	22.7	18.9
Dy^{162}	1.72	1.98	22.2	25.5
Dy^{163}	1.07	1.09	2.9	24.9
Dy^{164}	1.78	1.27	14.0	28.1

Ho^{165}	1.00	1.65		100
Er^{162}		1.51	6.3	.14
Er^{164}	1.01	2.08	24.1	1.6
Er^{166}	1.48	1.84	13.8	33.4
Er^{167}	.73	2.36	45.8	22.9
Er^{168}	1.63	1.26	8.5	27.1
Er^{170}	.84	.69	1.4	14.9
Tm^{169}	1.06	1.22		100
Yb^{168}		1.03	8.1	.14
Yb^{170}	.89	1.67	35.3	3.1
Yb^{171}	.85	.64	5.3	14.4
Yb^{172}	1.59	(3.02)	29.3	21.8
Yb^{173}	.76	1.23	12.8	16.2
Yb^{174}	.73	.72	4.1	31.6
Yb^{176}	.83		5.1	12.6
Lu^{175}	1.06	1.07	100	97.4
Lu^{176}			0	2.6
Hf^{174}			0	.16
Hf^{176}	.88	(1.93)	7.1	5.2
Hf^{177}	.99	(1.79)	9.2	18.6
Hf^{178}	1.29	(1.83)	18.4	27.1
Hf^{179}	.60	1.60	37.5	13.8
Hf^{180}	1.47	.89	27.8	35.2

Ta^{180}			0	.01
Ta^{181}	.47	1.56	100	99.99
W^{180}	.42	.42	2.5	.14
W^{182}	1.43	(3.55)	25.3	26.4
W^{183}	1.29	1.23	18.3	14.4
W^{184}	1.41	1.14	24.2	30.6
W^{186}	1.50	.73	29.7	28.4
Re^{185}	1.01	1.24	72.0	37.1
Re^{187}	.83		28.0	62.9
Os^{184}		.95	6.9	.02
Os^{186}	.98	(1.86)	7.4	1.59
Os^{187}	.83	.53	5.3	1.64
Od^{188}	1.49	(2.17)	24.1	13.3
Os^{189}	1.24	1.00	13.5	16.1
Os^{190}	1.53	1.20	26.4	26.4
Os^{192}	1.32	1.11	16.3	41.0
Ir^{191}	.90	1.00	37.1	38.5
Ir^{193}	.49	1.23	62.9	61.5

Pt^{190}			0	.01
Pt^{192}	1.01	.93	8.3	.78
Pt^{194}	1.41	(2.68)	20.9	32.9
Pt^{195}	.97	1.52	27.0	33.8
Pt^{196}	1.59	1.14	31.7	25.2
Pt^{198}	1.17		12.1	7.2
Au^{197}	1.02	(2.02)		100
Hg^{196}	.52	1.50	23.6	.15
Hg^{198}	1.15	(2.32)	10.5	10.0
Hg^{199}	.96	(2.51)	6.8	16.8
Hg^{200}	1.58	(3.66)	28.4	23.1
Hg^{201}	1.40	(3.02)	18.8	13.2
Hg^{202}	1.16		10.8	29.8
Hg^{204}		.16	1.1	6.9
Tl^{203}	1.04	(1.4)	73.8	29.5
Tl^{205}	.59	(1.41)	26.2	70.5
Pb^{204}	.82	(3.93)	2.1	1.4
Pb^{206}	1.71	(5.13)	16.7	25.1
Pb^{207}	1.77	(4.21)	19.2	21.7
Pb^{208}	2.28	(5.01)	62.0	52.0

Bi^{209}	.76		100
Th^{232}	.47		100
U^{235}	.38	35.5	.72
U^{238}	.64	64.5	99.3

FIGURE CAPTIONS

Figure 1. Möbius loops.

Figure 2. Relative elemental abundances. Triangles, △, correspond to the present theoretical values. Open circles, ○, correspond to α^2CVn, a type Ap star(7), and dots, ●, represent Urey's tabulation of observed abundances(6).

Figure 3. A torus with equal radii.

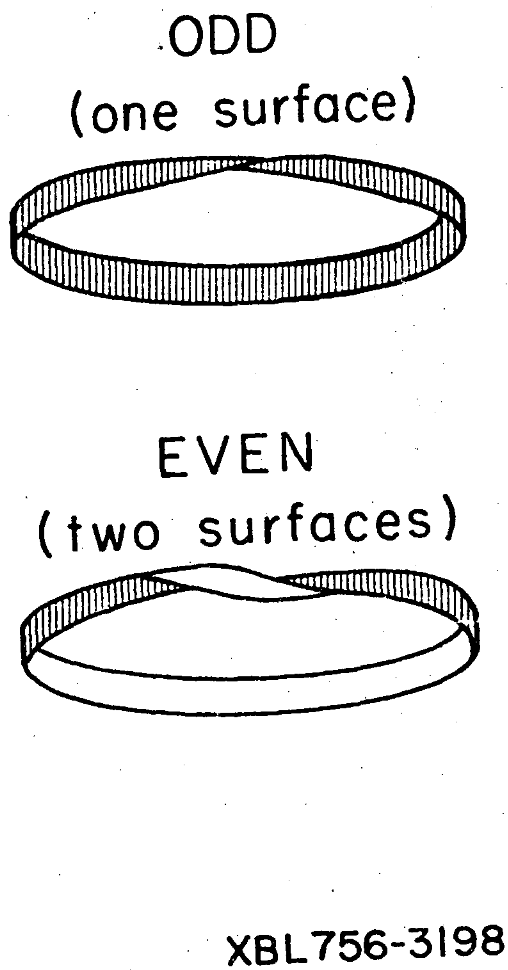

Figure 1

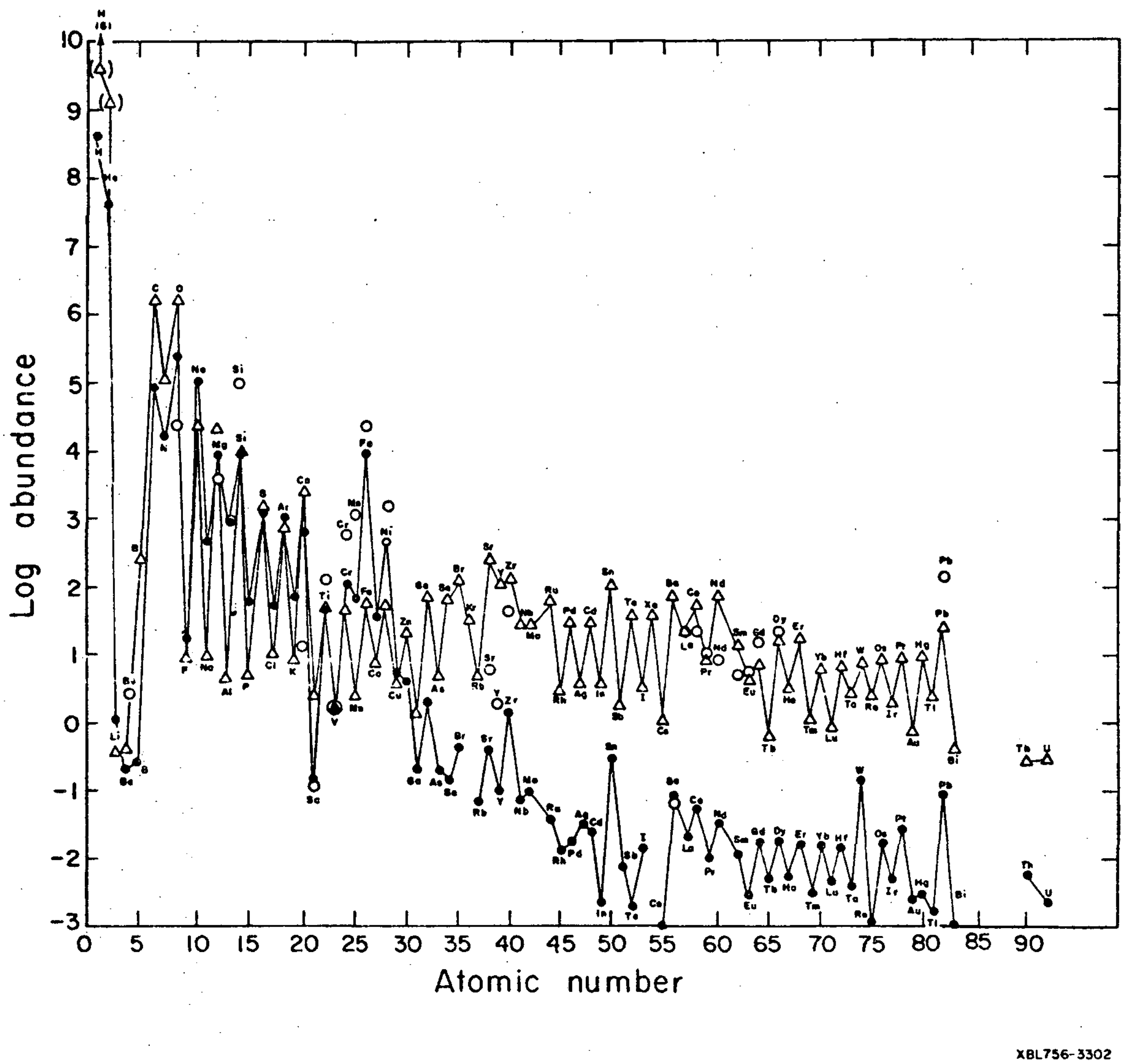

Figure 2

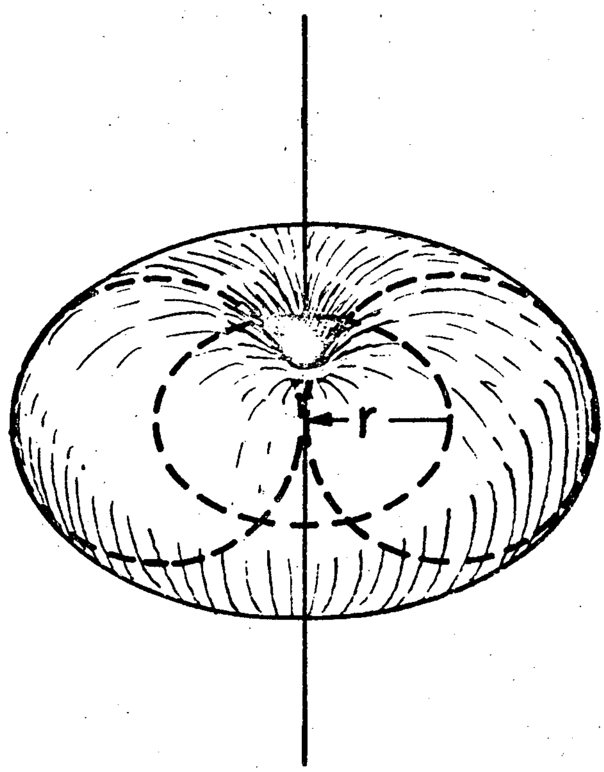

XBL759-4594

Figure 3

TECHNICAL INFORMATION DIVISION
LAWRENCE BERKELEY LABORATORY
UNIVERSITY OF CALIFORNIA
BERKELEY, CALIFORNIA 94720